

NiGe-Based Ohmic Contacts to n-Type GaAs

MASAKI FURUMAI, TAKEO OKU, HIDENORI ISHIKAWA,
AKIRA OTSUKI,* and YASUO KOIDE

Department of Materials Science and Engineering, Kyoto University,
Sakyo-ku, Kyoto 606-01, Japan

TETSUO OIKAWA

JEOL Ltd, 1-2 Musashino 3-chome, Akishima, Tokyo 196, Japan

MASANORI MURAKAMI

Department of Materials Science and Engineering, Kyoto University,
Sakyo-ku, Kyoto 606-01, Japan

Refractory NiGe ohmic contacts which have excellent thermal stability and smooth surface have been developed. To apply these contacts to the future very large scale integration GaAs devices, reduction of the contact resistance (R_c) of the NiGe contacts is mandatory. In the present paper, in order to obtain a guideline for the R_c reduction, the formation mechanism of the NiGe contacts was investigated. The NiGe contacts were found to have two different ohmic contact formation mechanisms. These mechanisms suggested that facilitation of heavy doping at the GaAs surface and/or in the Ge layer was very effective to reduce the R_c values of the NiGe contacts. Experimentally, the R_c reduction was demonstrated by adding a small amount of third elements. Direct doping elements (Sn, Sb, and Te) and indirect doping elements (Pd, Pt, Au, Ag, and Cu) were chosen as the third elements. In addition, the effect of addition of In, which forms a low barrier layer between metal and GaAs, was investigated. The contact resistance of these NiGe-based contacts were close to $0.3 \Omega \text{ mm}$, and they provided smooth surface and shallow reaction depth. Finally, the NiGe-based contacts were compared with the conventional AuGeNi contact.

Key words: NiGe, n-type GaAs, ohmic contact

INTRODUCTION

Development of thermally stable, low resistance ohmic contacts is mandatory for the progress of the GaAs device technology. Currently, AuGeNi ohmic contacts have been extensively used in the manufacturing of GaAs devices, because they provide low contact resistances ($\sim 0.1 \Omega \text{ mm}$) and their reproducibility is excellent.¹ However, these contacts have poor thermal stability, rough surface, rough interface, and deep diffusion depth to the GaAs substrate.²⁻⁴ In order to improve these undesirable properties of the AuGeNi contacts, non-gold Ge-based ohmic contacts such as

NiGe,⁵⁻⁷ NiGeWN,⁸ PdGe,^{9,10} and CuGe¹¹ contacts have been developed. However, the PdGe contacts showed thermal instability, and the CuGe contact showed deep diffusion of Cu into the GaAs substrate. Although the NiGeWN had excellent thermal stability, it had a complicated fabrication process.

In our laboratory, the NiGe contacts with Ge concentrations of 13~43 at.% had been investigated,⁷ and were found to have excellent thermal stability at 400°C , smooth surface, and shallow reaction depth. However, the NiGe contacts yielded the relatively high contact resistance of $0.8 \Omega \text{ mm}$, and reduction of the contact resistance (R_c) by a factor of ~ 3 was necessary to use these contacts in the submicron devices.

The purpose of the present study is twofold. The first is to obtain a guideline for further reduction of

*Present address: Sumitomo Electric Industries Ltd., Osaka, Japan
(Received February 19, 1996; accepted July 1, 1996)

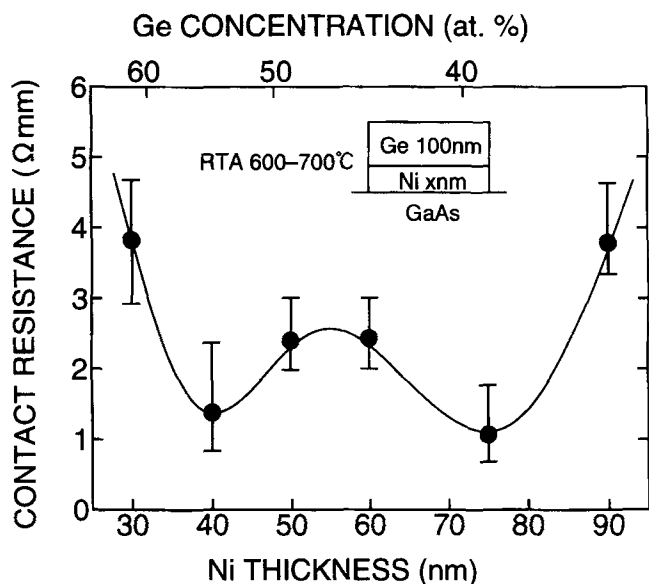


Fig. 1. Contact resistances of NiGe contacts with various Ni layer thicknesses.

the contact resistances by investigating the detailed formation mechanism of the binary NiGe contacts with wide Ge concentrations. The second purpose is to reduce the contact resistance of the NiGe contacts by adding a small amount of a third element, and to understand the ohmic contact formation mechanism. The electrical properties were investigated by a transmission line method (TLM), and the temperature dependence of the contact resistances was investigated in the temperature range between -191 and 92°C . The sample preparation procedure is similar to that of the preceding paper.¹²⁻¹⁴ The interfacial microstructures of the contacts were analyzed by x-ray diffraction (XRD), high-resolution electron microscopy (HREM), and energy dispersive x-ray spectroscopy (EDX). These studies will construct a model for ohmic contact formation of the NiGe-based ohmic contacts.

FORMATION MECHANISM OF NiGe OHMIC CONTACTS

In this section, formation mechanism of NiGe ohmic contacts was investigated by correlating the electrical properties to the interfacial microstructure in order to obtain a guideline for reduction of contact resistances.

Dependence of the R_c values on the Ni layer thickness of the NiGe contacts was investigated to search the optimum Ni thickness to provide the minimum R_c value. The R_c values of the Ni(x nm)/Ge(100 nm) contacts annealed at temperatures around $600\text{--}700^{\circ}\text{C}$ for 5 s are plotted in Fig. 1 as a function of the Ni layer thickness. Ohmic behavior was observed in the contacts with the Ni layer thickness in the range of 40 to 75 nm. (The Ni(30 nm)/Ge(100 nm) and Ni(90 nm)/Ge(100 nm) contacts showed ohmic-like behavior.) W-shaped dependence of R_c values on the Ni layer thickness is observed as shown in Fig. 1, which had been also observed by Ohata and Ogawa,⁵ and the minimum R_c values are obtained at the Ni layer thick-

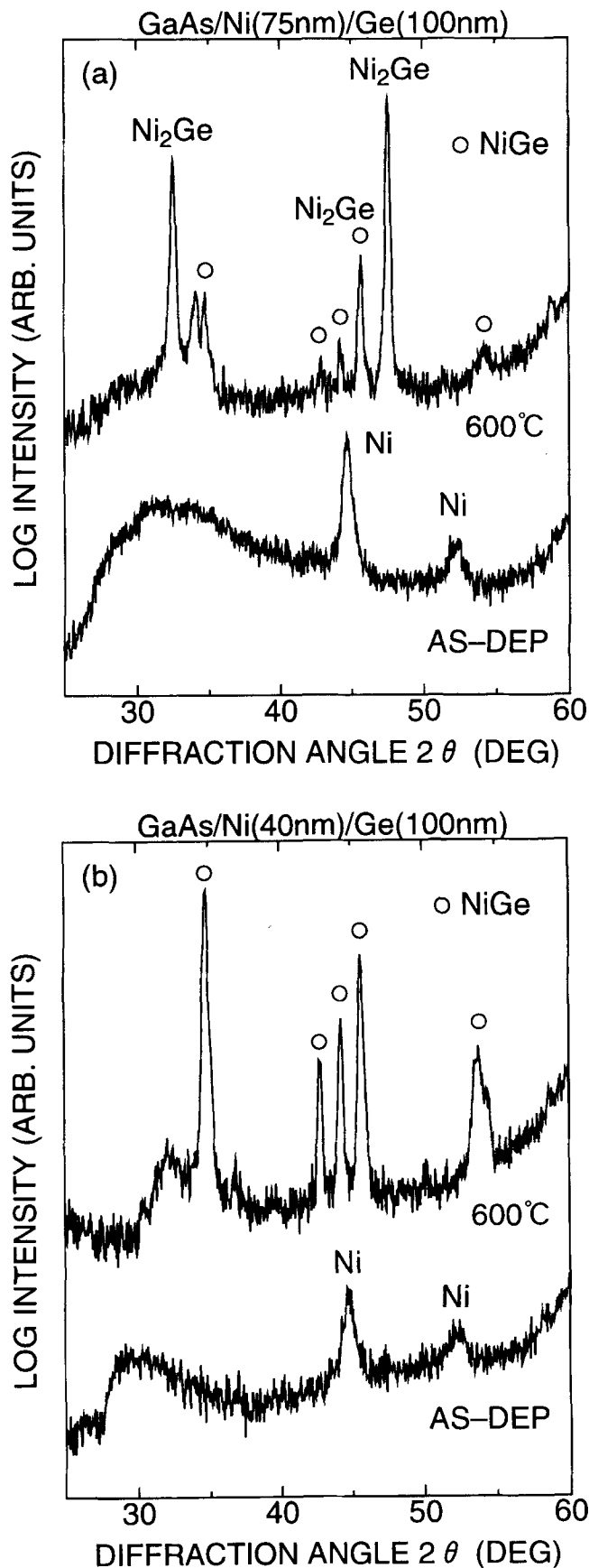


Fig. 2. Changes of XRD profiles of (a) Ni(75 nm)/Ge(100 nm) and (b) Ni(40 nm)/Ge(100 nm) contacts before and after annealing.

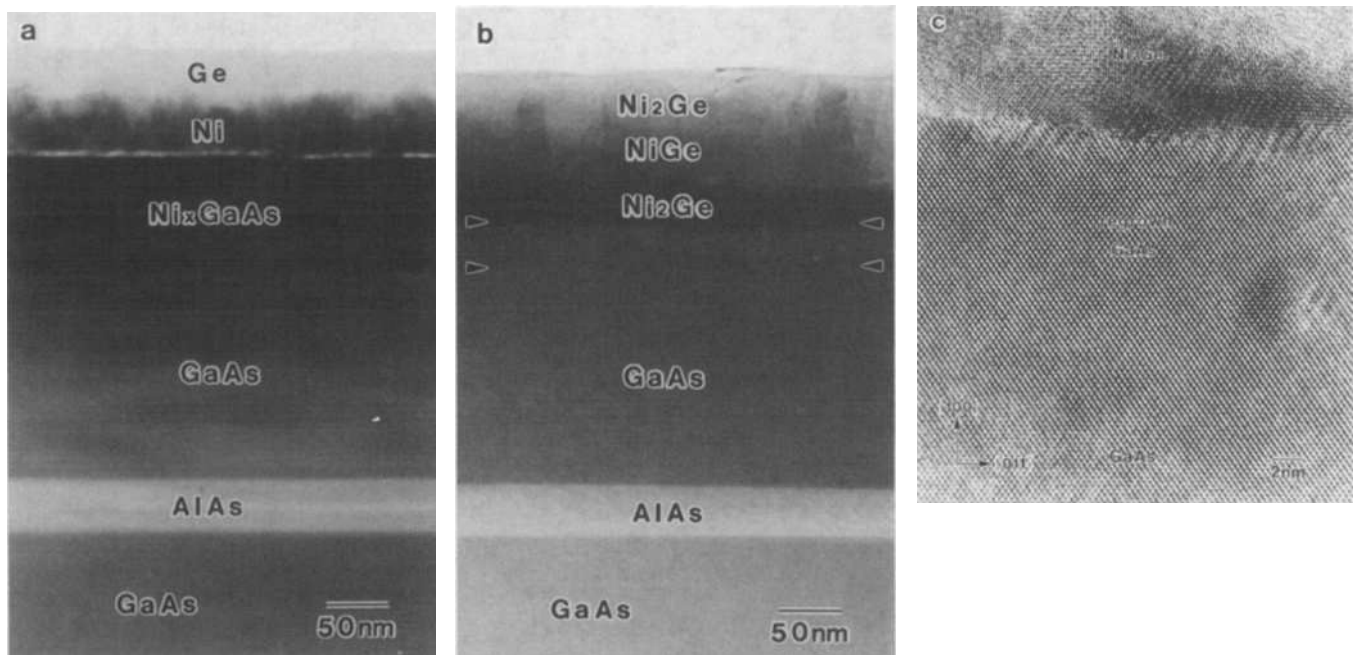


Fig. 3. (a) Low magnification image and (b) high-resolution image of Ni(75 nm)/Ge(100 nm) contact annealed at 600°C for 5 s, taken with the incident beam parallel to the $[0\ \bar{1}\ 0]$ of the GaAs substrate. (c) EDX spectra at the GaAs surface.

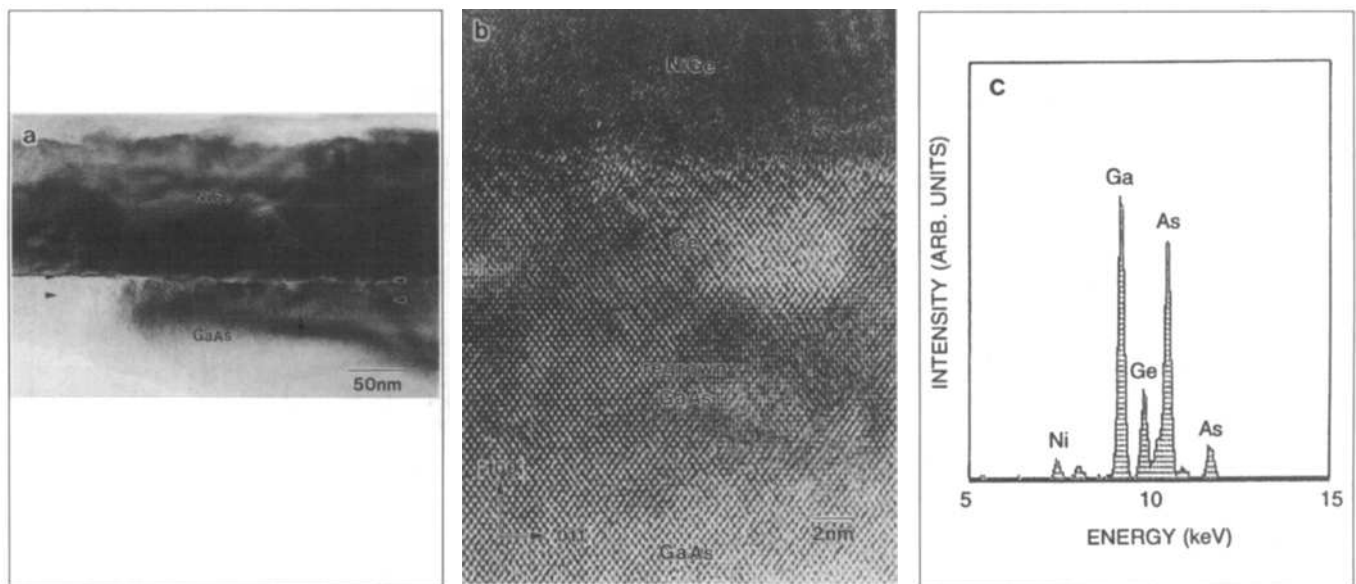


Fig. 4. (a) Low magnification image and (b) high-resolution image of Ni(40 nm)/Ge(100 nm) contact annealed at 600°C for 5 s, taken with the incident beam parallel to the $[0\ \bar{1}\ 0]$ of the GaAs substrate. (c) EDX spectra at the GaAs surface.

nesses of 40 and 75 nm after annealing at $\sim 600^\circ\text{C}$. The metal sheet resistances were measured to be about $6\ \Omega/\square$ in the Ni(75 nm)/Ge(100 nm) contact, and decreased down to $3\ \Omega/\square$ in the Ni(40 nm)/Ge(100 nm) contact.

To investigate thermal stability after contact formation, isothermal annealing was carried out. The Ni(75 nm)/Ge(100 nm) and Ni(40 nm)/Ge(100 nm) contacts were stable after annealing at 400°C for 3 h, and the surface morphology was smooth after annealing at 400°C for 10 h.

Figure 2 shows XRD profiles of (a) Ni(75 nm)/Ge(100 nm) and (b) Ni(40 nm)/Ge(100 nm) contacts

which provided the minimum R_c values after annealing at 600°C . In the as-deposited samples, several XRD peaks corresponding to Ni are observed, indicating that the Ni layer has a polycrystalline structure. No XRD peaks corresponding to Ge were detected, indicating that the Ge layer has an amorphous structure. After annealing at 600°C for 5 s, Ni_2Ge and NiGe compounds are detected for the Ni(75 nm)/Ge(100 nm) contact as shown in Fig. 2a. On the other hand, only NiGe compounds are detected for the Ni(40 nm)/Ge(100 nm) contact after annealing at 600°C as shown in Fig. 2b.

To observe directly the microstructure at the GaAs/

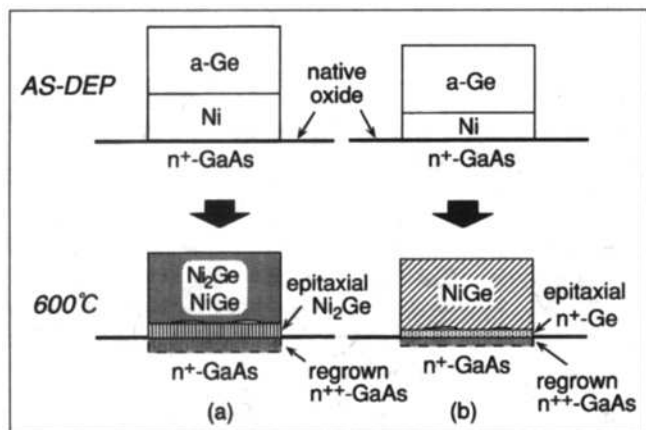


Fig. 5. Schematic illustration at GaAs/metal interface of NiGe contacts with the minimum R_c values. (a) Ni(75 nm)/Ge(100 nm), and (b) Ni(40 nm)/Ge(100 nm) contacts, where a-Ge represents amorphous Ge.

metal interface, HREM observation was performed for these contacts. Figures 3a and 3b are low magnification and high-resolution images, respectively, of the Ni(75 nm)/Ge(100 nm) contact annealed at 600°C for 5 s. After annealing at 600°C, Ni atoms react with Ge forming Ni_2Ge and NiGe compounds as shown in Fig. 3a. The GaAs surface is covered by the Ni_2Ge compounds which were identified by EDX analysis (Ni:Ge = 65:35). Dark contrast around the GaAs surface indicated by arrows in Fig. 3a is due to formation of a regrown GaAs layer. Thickness of the regrown GaAs is ~20 nm, which is shallow reaction depth. A thin native oxide layer, which existed on the GaAs surface before annealing, is observed locally between the epitaxial- Ni_2Ge layer and polycrystalline NiGe compounds layer. An enlarged high-resolution image of the GaAs/ Ni_2Ge interface is shown in Fig. 3b. Although a small grain with weak contrast is observed in the regrown GaAs layer, the regrown layer has no observable defects and precipitates. The Ni_2Ge layer is epitaxially grown on the regrown GaAs. The {102} and {110} planes of the Ni_2Ge are parallel to the {110} GaAs.

Figures 4a and 4b are low magnification and high-resolution images, respectively, of the Ni(40 nm)/Ge(100 nm) contact annealed at 600°C for 5 s. After annealing at 600°C, Ni atoms react with Ge forming NiGe compounds as shown in Fig. 4a. The GaAs surface is covered by the NiGe compounds which were determined by EDX analysis. Dark contrast around the GaAs surface indicated by arrows is due to formation of a regrown layer. Thickness of the reaction depth is ~20 nm. A thin native oxide layer is observed locally at the interface. An enlarged high-resolution image at the interface of Fig. 4a is shown in Fig. 4b. At the interface between the regrown GaAs and NiGe compounds, a thin epitaxial Ge layer with the thickness of ~8 nm is observed. There are no defects at the regrown GaAs/Ge interface because they have almost the same lattice constants ($a_{GaAs} = 0.5653$ nm, $a_{Ge} = 0.5646$ nm).¹⁵ The Ge layer is detected by EDX analysis as shown in Fig. 4c. A K_{α} peak corresponding to Ge

is observed at 9.8 keV. (No peaks corresponding to Cu were observed because a beryllium sample holder was used in this experiment.)

The NiGe contacts have two different interfacial structures, which is different from other Ge-based contacts such as PdGe¹⁰ and CuGe¹¹ contacts. Here, the microstructures of the NiGe contacts with the minimum R_c values deduced from the present XRD, HREM, and EDX results are discussed.

The interfacial reactions in the Ni(75 nm)/Ge(100 nm) contact with low Ge concentration (39 Ge at.%) and Ni(40 nm)/Ge(100 nm) contact with high Ge concentration (55 Ge at.%) will be discussed by referring to Figs. 5a and 5b, respectively. In the Ni(75 nm)/Ge(100 nm) contact, a small fraction of Ni reacts with GaAs to form Ni_xGaAs compounds⁶ at the initial stages of annealing (<300°C). At elevated temperatures of 600°C, Ni in the Ni_xGaAs reacts with Ge forming Ni_2Ge and NiGe compounds, and the regrown GaAs layer forms as shown in Fig. 5a. The GaAs surface is covered by the epitaxially grown Ni_2Ge compound, and the polycrystalline Ni_2Ge and NiGe compounds are formed in the layer close to the contact surface.

A volume ratio of Ni_2Ge to NiGe was estimated to be about 9:1 from the present XRD and HREM results, and a small amount of Ge remained unreacted in the contact metal. It is believed that a small amount of Ge atoms would diffuse in the regrown GaAs layer, resulting in formation of a Ge-doped n^{++} -GaAs layer by substituting the Ga with the Ge atoms. Although no Ga compounds were detected by the present XRD, the dissociated Ga atoms might diffuse in the NiGe layer. The Ge-doped n^{++} -layer facilitates carrier tunneling probability, transiting Schottky behavior to ohmic behavior, which results in reduction of the contact resistance.

The interfacial reaction of the Ni(40 nm)/Ge(100 nm) contact is discussed by referring to Fig. 5b. At the initial stages of annealing (<300°C), a small fraction of Ni reacts with GaAs to form Ni_xGaAs compounds.⁷ At elevated temperatures of 600°C, Ni in the Ni_xGaAs reacts with Ge, forming NiGe compound, and the regrown GaAs and the epitaxial Ge layers are formed as shown in Fig. 5b. Since the NiGe compounds are formed on the GaAs surface, a small amount of the excess Ge atoms remains unreacted in the contact metal. These Ge atoms form an epitaxial n^{++} -Ge layer which would be heavily doped with As decomposed from the GaAs surface upon the high temperature annealing. In addition, it is believed that a small amount of Ge atoms diffuse in the regrown GaAs layer, resulting in formation of a Ge-doped n^{++} -GaAs layer. Thus, the Ni(40 nm)/Ge(100 nm) contact has the interface structure of n^{++} -GaAs/ n^{++} -GaAs/ n^{++} -Ge/metal, which provides the ohmic behavior.

These ohmic contact formation mechanisms of NiGe contacts suggest that the further reduction of the R_c values will be achieved by facilitating additional doping at the GaAs surface and/or in the epitaxially grown Ge layer.

EFFECTS OF ADDITION OF THIRD ELEMENTS TO NiGe CONTACTS

Role of Third Elements

Further studies to reduce the contact resistance without deteriorating the thermal stability of the NiGe contacts by adding a small amount of third elements were investigated. The third elements should increase the donor concentration at the GaAs surface or Ge layer and/or form an intermediate semiconductor layer which has low energy barrier height to the contact metals.

To increase the donor concentration, direct doping elements and indirect doping elements were chosen as the third elements. The "direct" doping elements are Sn, Sb, and Te which will increase the donor concentration directly at the GaAs surface or Ge layer. The "indirect" doping elements are Pd, Pt, Au, Ag, and Cu. To increase the donor concentration (Ge or As) at the GaAs surface or Ge layer, the third elements (M) must form M-Ga phases at the GaAs surface, so that the donor atoms can easily diffuse to the Ga vacancies in the vicinity of the semiconductor surface. The mixing enthalpy of the element M with Ga should be smaller than that with As, and these metals are Pd, Pt, and Au.¹⁶ Formation of a small volume fraction of M-Ga phases will facilitate heavy Ge or As doping at the GaAs or Ge surface, which is expected to reduce the R_c values. In addition, Ag and Cu have wide solubility with Ga in a wide temperature range, forming M(Ga) solid solutions.¹⁷ The formation of the M(Ga) solid solutions will increase the Ga vacancy concentration, and facilitate heavy doping of Ge atoms at the GaAs surface.

To form an intermediate layer with low energy barrier, an addition of a small amount of In to the NiGe is desirable. Indium is expected to form an intermediate $\text{In}_x\text{Ga}_{1-x}\text{As}$ layer with low energy barrier between the metal and the GaAs substrate, leading to reduction of the contact resistances.

The effects of addition of Au, Ag, and In had been previously investigated in our laboratory.¹²⁻¹⁴ The addition of the third element thinner than 6 nm reduced the contact resistance down to 0.3 Ω mm which barely satisfied the requirement for 1 μm metal-semiconductor field-effect transistor (MESFET) devices. In addition, these contacts had smooth surface and shallow reaction depth, and the NiGe(Au) and NiGe(In) showed excellent thermal stability at 400°C for 3 h. (Note that the contact with a small amount of a third element (M) is denoted as the "NiGe(M)" contact in this paper.) However, further reduction of the contact resistance is required for the future sub-micron devices. Therefore, the effects of addition of "direct" doping elements (Sn, Sb, and Te) and "indirect" doping elements (Pd, Pt, and Cu) were investigated and the results will be given in the next sections.

Since the contact resistance and thermal stability of the NiGe-based ohmic contacts were previously found

to be very sensitive to the Ni and Ge atomic ratio ($X_{\text{Ni}}/X_{\text{Ge}}$) as shown in Fig. 1, the addition of the third elements to NiGe contacts would influence the optimum $X_{\text{Ni}}/X_{\text{Ge}}$ ratios to provide the best contact properties. Therefore, a variety of the contacts with various Ni layer thicknesses were prepared, and two kinds of deposition sequences were used. Since Ni forms uniform Ni_xGaAs phase upon annealing at elevated temperatures⁷ and prevents the third element from diffusing into the GaAs substrate, samples with GaAs/Ni/M/Ge or GaAs/M/Ni/Ge (M = Sn, Sb, Te, Pd, Pt, and Cu) structure were prepared. (A sign "/" indicates the sequential deposition.)

Reduction of R_c by Adding a Third Element

The dependences on the annealing temperatures and the Ni thickness on the electrical properties of NiGe(M) (M = Sn, Sb, Te, Pd, Pt, and Cu) contacts were studied.

Figure 6a shows the contact resistances of the Sn(6 nm)/Ni(40 nm)/Ge(100 nm), Ni(40 nm)/Sb(6 nm)/Ge(100 nm)/

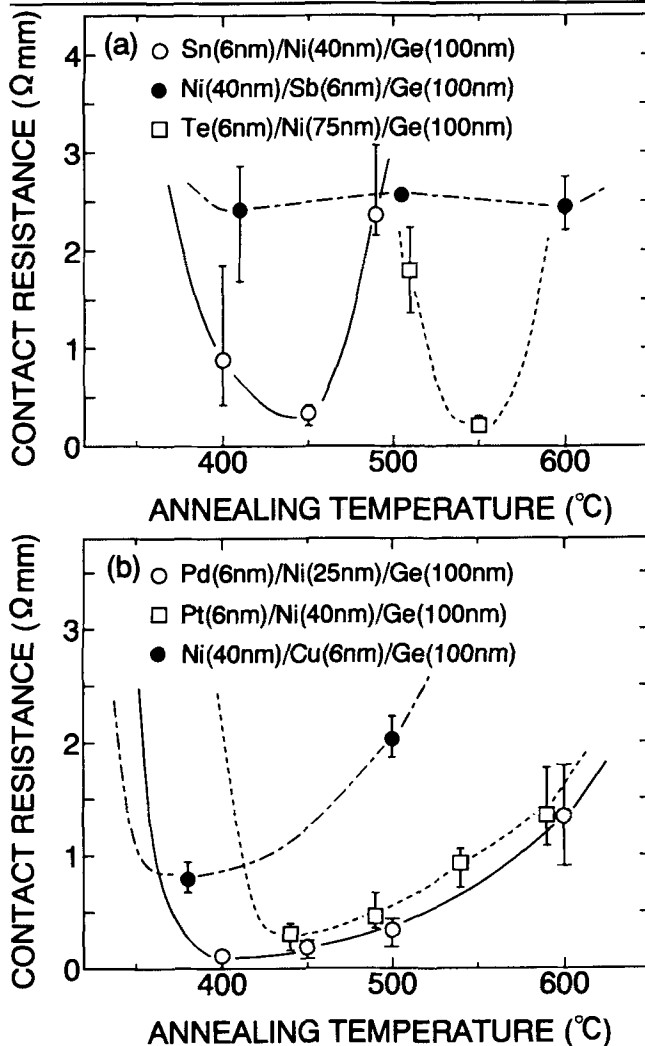


Fig. 6. Contact resistances of (a) Sn(6 nm)/Ni(40 nm)/Ge(100 nm), Ni(40 nm)/Sb(6 nm)/Ge(100 nm) and Te(6 nm)/Ni(75 nm)/Ge(100 nm) contacts, and (b) Pd(6 nm)/Ni(25 nm)/Ge(100 nm), Pt(6 nm)/Ni(40 nm)/Ge(100 nm) and Ni(40 nm)/Cu(6 nm)/Ge(100 nm) contacts annealed at various temperatures for 5 s.

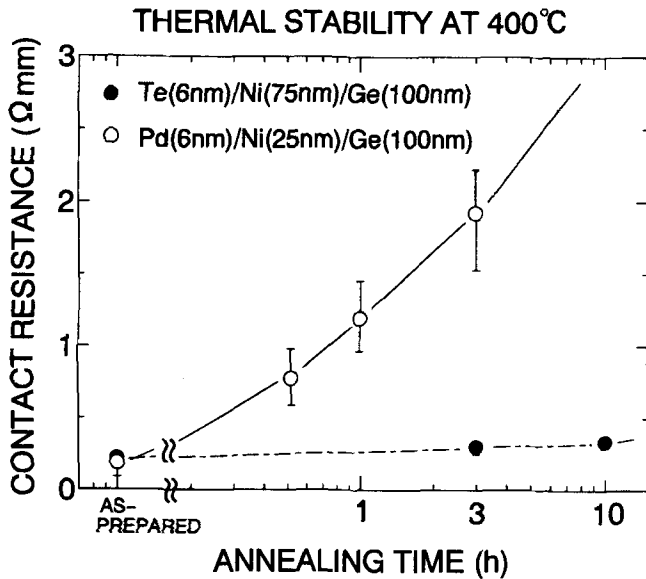


Fig. 7. Changes of contact resistance of Te(6 nm)/Ni(75 nm)/Ge(100 nm) and Pd(6 nm)/Ni(25 nm)/Ge(100 nm) contacts during isothermal annealing at 400°C.

Ge(100 nm), and Te(6 nm)/Ni(75 nm)/Ge(100 nm) contacts as a function of annealing temperatures. For the direct doping element (Sn, Sb, and Te) addition, the temperature-Ni thickness regions, in which the ohmic behavior was observed, were narrow. The error bars indicate the highest and lowest R_c values among ten TLM measurements, respectively. In the NiGe(Sn) contact, the lowest R_c values of 0.34 Ω mm (which corresponds to the specific contact resistance of $4.8 \times 10^{-6} \Omega \text{ cm}^2$) with minimum R_c spread was obtained after annealing at 450°C for 5 s. In the NiGe(Sb) contact, the R_c values of $\sim 2 \Omega$ mm were obtained at temperatures in the range of 400 ~ 600°C. In the NiGe(Te) contact, the lowest R_c value of 0.21 Ω mm (corresponding to $1.8 \times 10^{-6} \Omega \text{ cm}^2$) was obtained after annealing at 550°C for 5 s. The metal sheet resistances (R_s) of the NiGe(Sn) and NiGe(Te) contacts were $\sim 3 \Omega/\square$ and $\sim 2 \Omega/\square$, respectively.

Figure 6b shows the contact resistances of the Pd(6 nm)/Ni(25 nm)/Ge(100 nm), Pt(6 nm)/Ni(40 nm)/Ge(100 nm), and Ni(40 nm)/Cu(6 nm)/Ge(100 nm) contacts as a function of annealing temperatures. For the indirect doping element (Pd, Pt, and Cu) addition, the temperature-Ni thickness regions, in which the ohmic behavior was observed, were wide. In the NiGe(Pd) contact, the lowest R_c value of 0.12 Ω mm (corresponding to $6.3 \times 10^{-7} \Omega \text{ cm}^2$) was obtained after annealing at 400°C for 5 s. In the NiGe(Pt) contact, the lowest R_c value of 0.31 Ω mm (corresponding to $4.4 \times 10^{-6} \Omega \text{ cm}^2$) was obtained after annealing at 450°C for 5 s. The lowest R_c value of 0.8 Ω mm was obtained after annealing at 400°C for 5 s in the NiGe(Cu) contact. The metal sheet resistances (R_s) of the NiGe(Pd) and NiGe(Pt) contacts were $\sim 5 \Omega/\square$ and $\sim 3 \Omega/\square$, respectively.

To investigate the thermal stability after contact formation, isothermal annealings at temperatures in the range of 300 to 400°C were carried out for the

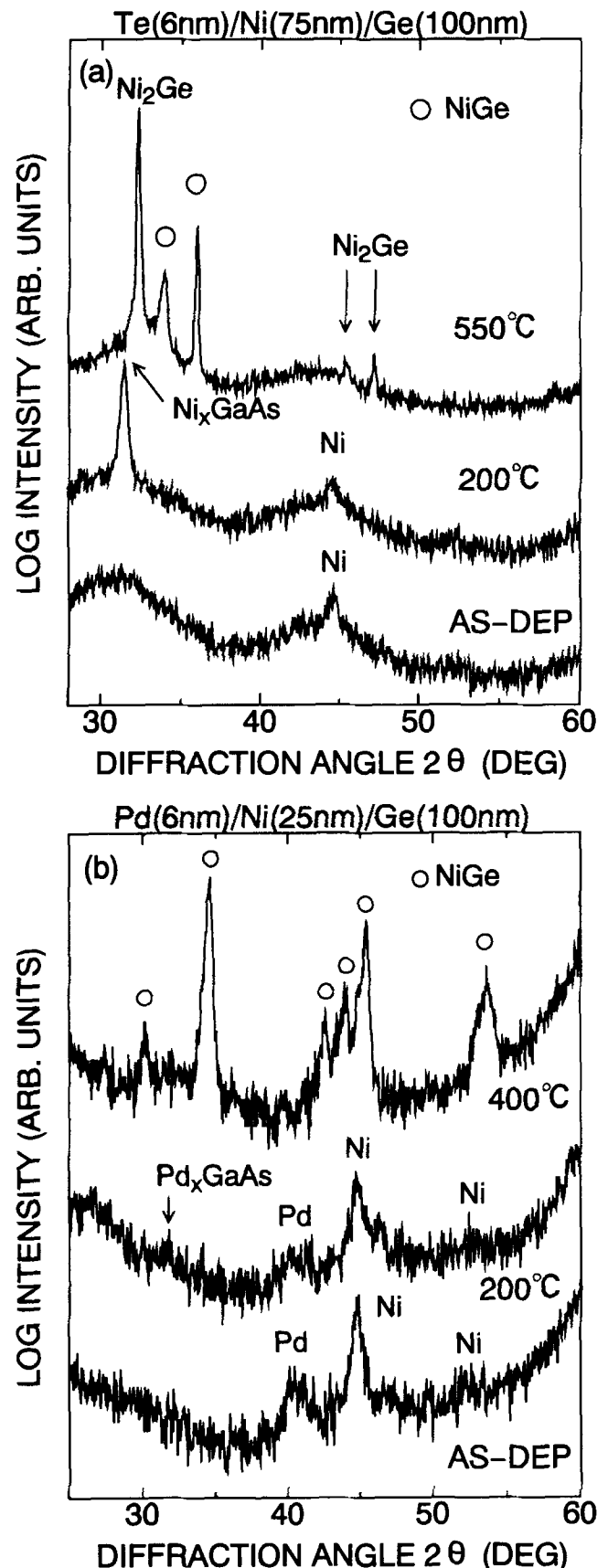


Fig. 8. Changes of XRD profiles of (a) Te(6 nm)/Ni(75 nm)/Ge(100 nm), and (b) Pd(6 nm)/Ni(25 nm)/Ge(100 nm) contacts before and after annealing.

NiGe(Te) and NiGe(Pd) contacts prepared by annealing at 550 and 400°C for 5 s, which provided the lowest R_c values. The R_c values of the NiGe(Te) and NiGe(Pd) contacts are shown in Fig. 7 as a function of annealing times. In the NiGe(Te) contact, the R_c value increased slightly with increasing annealing times and is 0.3 Ω mm after annealing for 10 h. This contact has very good thermal stability. In the NiGe(Pd) contact, the R_c value increased by a factor of ~ 10 after annealing for 3 h. However, the R_c value of NiGe(Pd) contact showed excellent thermal stability during annealing at 300°C for 10 h.

Formation Mechanism of NiGe Contacts with a Third Element

The microstructures at the GaAs/metal interfaces were investigated by XRD, Rutherford backscattering (RBS), HREM, and EDX to understand the contact formation mechanism of the NiGe(Te) and NiGe(Pd) contacts which provided the lowest R_c values. Figure 8 shows XRD profiles of the (a) NiGe(Te) and (b) NiGe(Pd) contacts before and after annealing. XRD peaks corresponding to the Ni and Pd layers are observed in the as-deposited samples. No diffraction peak from Ge is observed, indicating that the Ge layer would have amorphous structure. Te was not detected by XRD due to the volume fraction below the detection limit. Upon annealing these samples at temperatures higher than 200°C, the microstructure of the NiGe(Te) contact is clearly different from that of the NiGe(Pd) contact. In the NiGe(Te) contact, a fraction of Ni reacts with the GaAs substrate growing a ternary Ni_xGaAs compound layer¹⁸⁻²⁰ epitaxially on the GaAs substrate after annealing at 200°C, as shown in Fig. 8a. After annealing at 550°C, the Ni_2Ge layer and polycrystalline NiGe layer are detected, in which the contact provided the lowest R_c value of 0.21 Ω mm. In the NiGe(Pd) contact, a fraction of Pd reacts with the GaAs substrate forming a ternary Pd_xGaAs ²⁰⁻²² compounds after annealing at 200°C, as shown in Fig. 8b. After annealing at 400°C, only NiGe compounds are detected, where the contact provided the lowest R_c value of 0.12 Ω mm.

The atomic distributions of the NiGe(Te) and NiGe(Pd) contacts perpendicular to the GaAs substrate were investigated by RBS. Figure 9a shows RBS spectra of the NiGe(Te) contact. For the as-deposited sample, no spectrum corresponding to Te was detected, which indicates that the energy peaks corresponding to the Ge and Te superimpose in the range of 1.57 ~ 1.62 MeV. After annealing at 200°C, the low energy edge of the Ni spectrum shifts to the lower side (as indicated by a star mark), which indicates the Ni diffusion into the GaAs substrate and the formation of the Ni_xGaAs layer. After annealing at 550°C, the Ni spectrum shifts back to the higher energy side, and the Ge spectrum shifts to the lower energy side, which indicates the formation of NiGe compounds. However, the energy peak corresponding to Te does not shift to the higher energy side, which indicates that the Te atoms remain at the GaAs

surface. Figure 9b shows RBS spectra of the NiGe(Pd) contact. For the as-deposited sample, the energy peaks corresponding to Ge and Pd elements superimpose in the range of 1.56 ~ 1.62 MeV. There is little change in the spectra after annealing at 200°C, which indicates the shallow reaction depth. After annealing at 400°C, the energy peak corresponding to Pd shifts

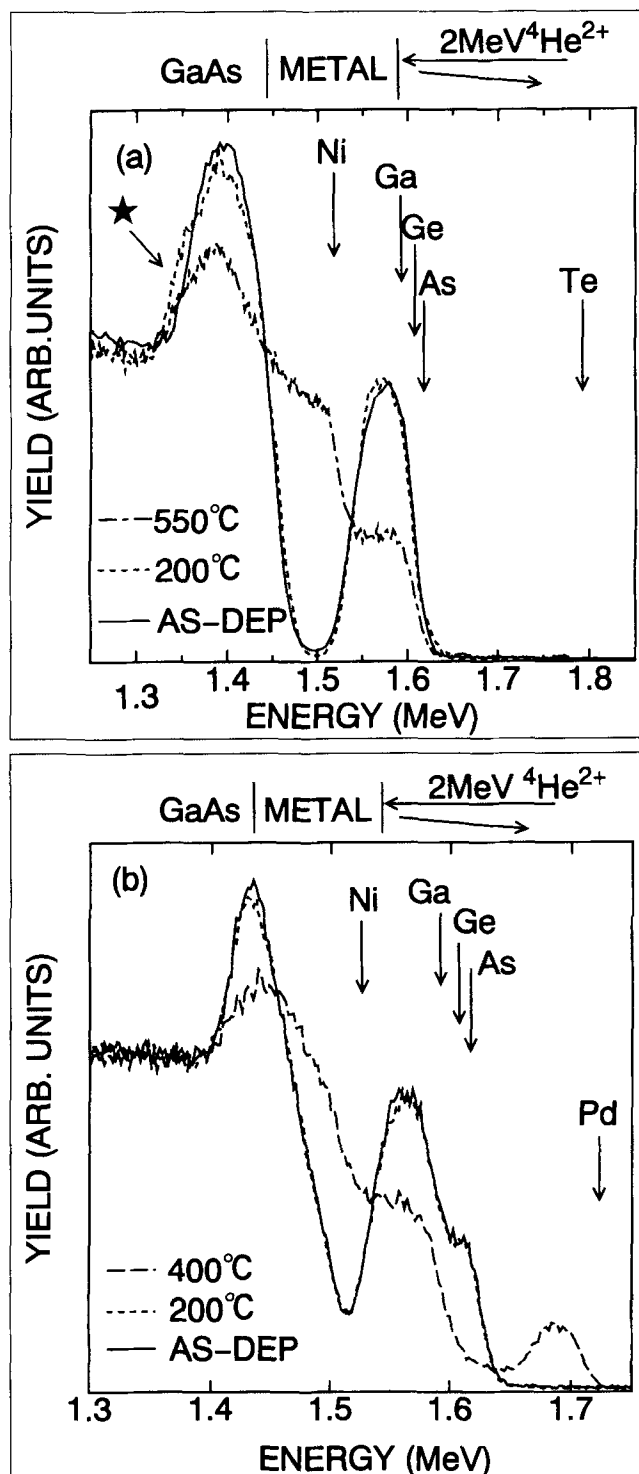


Fig. 9. Changes of RBS spectra of (a) Te(6 nm)/Ni(75 nm)/Ge(100 nm), and (b) Pd(6 nm)/Ni(25 nm)/Ge(100 nm) contacts before and after annealing.

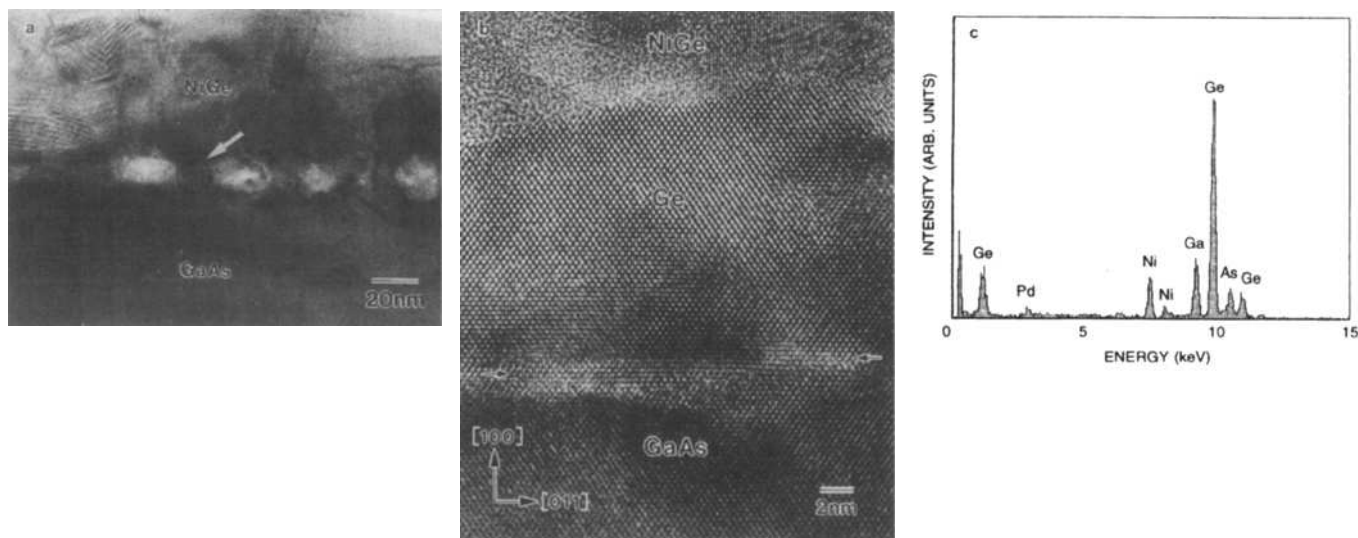


Fig. 10. (a) Low magnification image and (b) high-resolution image of Pd(6 nm)/Ni(25 nm)/Ge(100 nm) contact annealed at 400°C for 5s, taken with the incident beam parallel to the $[0\ \bar{1}\ 0]$ of the GaAs substrate. (c) EDX spectra between NiGe and GaAs substrate.

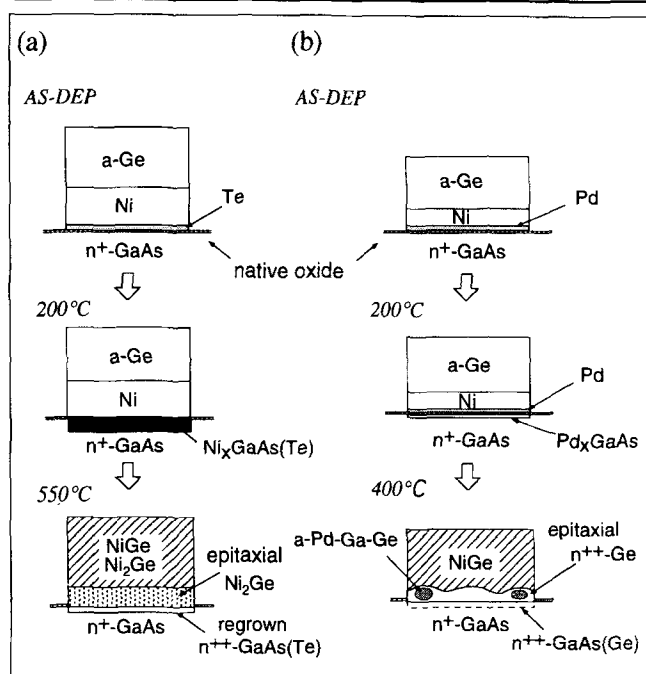


Fig. 11. Schematic illustrations of microstructure at GaAs/metal interface of (a) NiGe(Te) and (b) NiGe(Pd) contacts, where a-Ge represents amorphous Ge.

to ~ 1.69 MeV, which indicates Pd diffuse to the contact surface. The spectrum shifts of Ni and Ge indicate the formation of NiGe compounds.

The microstructure at the GaAs/metal interface was observed by HREM and EDX for the NiGe(Pd) contact which provided the lowest contact resistance of $0.12\ \Omega\ \text{mm}$. Figures 10a and 10b are a low magnification and high-resolution images of the contact annealed at 400°C for 5 s, respectively. The Ni layer reacts with Ge forming the NiGe compounds as shown in Fig. 10a. Thickness of the reaction depth is ~ 10 nm. An enlarged high-resolution image of the interface area marked by a circle in Fig. 10a (which would be the main electron transport path) is shown in Fig.

10b, where an epitaxial relation between the Ge and GaAs substrate ($\text{Ge}(001)\parallel\text{GaAs}(001)$) is observed. The Ge layer thickness is measured to be in the range of 2–20 nm. The EDX spectra at the interface area marked by a circle in Fig. 10a is also shown in Fig. 10c. In this figure, a strong K_{α} peak from Ge is detected, which shows the existence of a polycrystalline Ge layer. The EDX results also showed that the amorphous phase with white contrast at the NiGe/GaAs interface shown in Fig. 10a is the Pd-Ga-Ge phase. The microstructural change of the NiGe(Pd) contact, which was believed to cause the electrical instability during isothermal annealing at 400°C after contact formation, was also investigated by HREM. A thick (30 nm) uniform epitaxial Ge layer grown on the GaAs, and the amorphous Pd-Ga-Ge phases partially transformed to polycrystalline Pd_5Ga_2 compounds.

Based on these microstructural analyses, we will discuss the ohmic contact formation mechanisms of the NiGe(Te) and NiGe(Pd) contacts.

Schematic illustrations of the microstructural change of the NiGe(Te) and NiGe(Pd) contacts before and after annealing are shown in Figs. 11a and 11b, respectively. For the as-deposited sample, a very thin native oxide layer exists at the GaAs/metal interface.² At the initial stages of annealing at 200°C in the NiGe(Te) contact, a fraction of Ni atoms reacts with the GaAs substrate forming a ternary Ni_xGaAs layer which would contain the Te atoms. No reaction is observed between the amorphous Ge and Ni layer. After annealing at 550°C, the Ni atoms diffuse back to the Ge layer forming NiGe and Ni_2Ge compounds. The decomposition of the Ni_xGaAs layer results in the epitaxial regrowth of a GaAs layer on the GaAs substrate, and the Te atoms would be doped at the As sites in the “regrown” GaAs layer. Therefore, the R_c reduction is believed to be due to formation of the heavily doped $n^{++}\text{-GaAs}$ layer at the GaAs/metal interface, and that the majority of carriers transport through the $n^{+}\text{-GaAs}/n^{++}\text{-GaAs}/\text{metal}$ interface. The

cross-sectional structure is schematically shown in Fig. 11a.

After annealing at 200°C in the NiGe(Pd) contact, a fraction of Pd atoms reacts with the GaAs substrate forming a Pd_xGaAs layer. After annealing at 400°C, the Ni layer reacts with the Ge layer forming NiGe compounds. The excess Ge diffuse through the NiGe compounds to grow epitaxially on the GaAs substrate due to excellent lattice match with GaAs. The Ga atoms in the Pd_xGaAs layer react with Pd and excess Ge atoms, forming amorphous Pd-Ga-Ge in the epitaxial Ge layer. The formation of Pd-Ga-Ge phase leaves the excess As atoms in the epitaxial Ge layer, resulting in heavy doping of the Ge layer with As atoms. In addition, the GaAs surface is believed to be doped with Ge atoms diffused from the epitaxial Ge layer. Therefore, the R_c reduction is believed to be due to the formation of the thin epitaxial n⁺⁺-Ge layer at the GaAs/metal interface, and that the majority of carriers transport through the n⁺-GaAs/n⁺⁺-GaAs/n⁺⁺-Ge/metal interface. The cross-sectional structure is schematically shown in Fig. 11b.

The thermal instability of the NiGe(Pd) contacts during annealing at 400°C may be due to reduction of the doping level at the n⁺⁺-Ge/metal interface at the elevated temperature. The reason is believed that Ga atoms in the Pd₅Ga₂ phases diffuse into the Ge layer and act as acceptors, which reduce the donor concen-

tration. To prevent the thermal degradation, a third element which forms thermally stable phases with Ga is desirable.

The R_c values of the NiGe(Te) contacts, which have

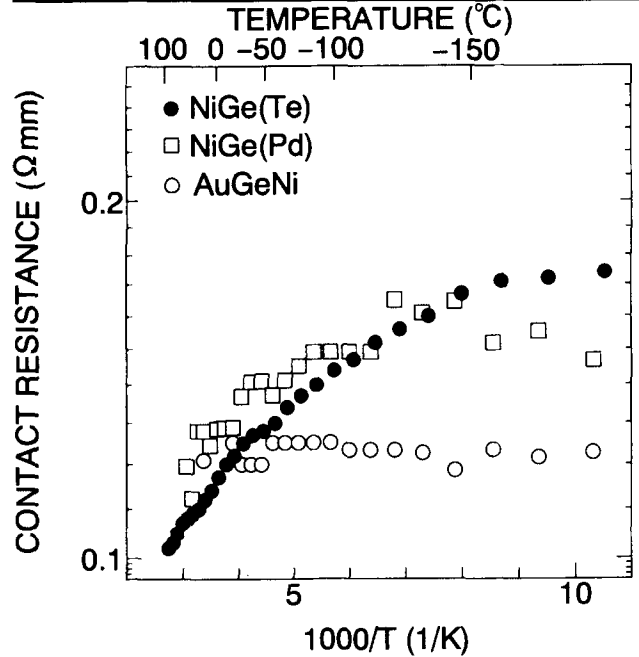


Fig. 12. Changes of contact resistance of NiGe(Te), NiGe(Pd), and AuGeNi contacts in temperature range between -196°C and 92°C.

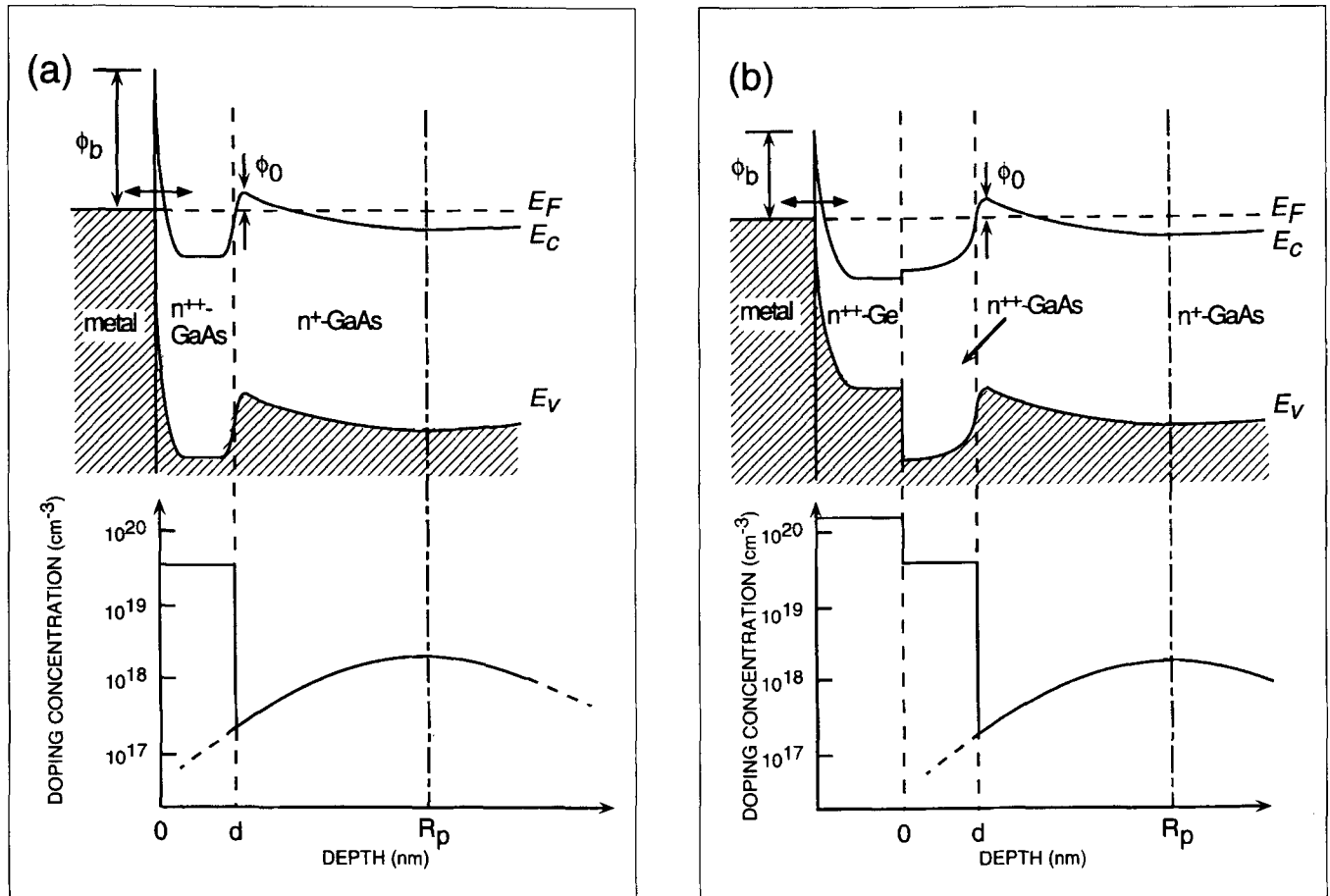


Fig. 13. Band diagrams and doping concentration profiles of (a) metal/GaAs and (b) metal/Ge/GaAs contacts.

Table I. The Properties of AuGeNi and NiGe-Based Contacts

	AuGeNi	NiGe	Direct Doping		Indirect Doping				Low Barrier
			NiGe(Sn)	NiGe(Te)	NiGe(Pd)	NiGe(Pt)	NiGe(Au)	NiGe(Ag)	NiGe(In)
Fabrication Process Window									
X _{Ni} /X _{Ge} Ratio	1~1.2	1.6	0.8	1.6	0.3~0.7	0.5~0.8	0.8	1.4~1.7	1.2~1.9
Annealing Temperature (°C)	400~550	600	450	550	400	450	450~550	550~650	600~700
Electrical Properties									
Contact Resistance (Ω mm)	0.1	0.8	0.3	0.2	0.1	0.3	0.2	0.3	0.3
Sheet Resistance (Ω/\square)	2	5	3	2	5	3	2	5	4
Thermal Stability at 400°C	Poor	Excellent	Poor	Good	Poor	Poor	Excellent	Poor	Excellent
Morphology									
Surface Morphology	Rough	Smooth	Smooth	Smooth	Smooth	Smooth	Smooth	Smooth	Smooth
Diffusion Depth (nm)	100	20	*	*	10	*	20	50	50

*Data not available.

no unstable compounds in the regrown GaAs layer, increased slightly (seen in Fig. 2) with increasing annealing times. This suggests a possibility of existence of a thermally equilibrium solubility limit of the donor concentration in the heavily doped n⁺⁺-layer. After contact formation, the donor concentration in the n⁺⁺-layer might be higher than the equilibrium concentration, and the excess donor atoms might diffuse out from the heavily doped layer upon annealing at 400°C, resulting in the increase of the R_c values. Further studies are needed to confirm the existence of the thermally equilibrium solubility of the donors in the heavily doped layer. In addition, the increase of R_c values may be due to reduction of surface states at the metal/semiconductor interface upon annealing at 400°C, which may increase the barrier height.

The surface morphology of the NiGe(M) (M = Sn, Sb, Te, Pd, Pt, and Cu) contacts was observed by optical microscopy. The surface was smooth and the edge profile was sharp, which is believed to be due to formation of the high melting point NiGe compounds (T_m ~850°C) close to the top surface. This morphology did not deteriorate after subsequent annealing at 400°C for 10 h.

Carrier Transport Mechanism of NiGe-Based Ohmic Contacts

To investigate the current transport mechanism of the NiGe(M) contacts, the R_c values were measured at temperatures in the range between -191 and 92°C for the NiGe(Te), NiGe(Pd), and the conventional AuGeNi contacts. The relations between the contact resistances and temperatures are shown in Fig. 12. All contacts provided the same R_c values of ~0.1 Ω mm at room temperature. For the NiGe(Te) and NiGe(Pd) contacts, the R_c values increase at low temperatures. Similar behavior was observed in the other NiGe-based ohmic contacts.¹³ On the other hand, the R_c value of the AuGeNi contact is independent on the temperatures. The R_c dependences of the NiGe(Te) and NiGe(Pd) contacts are clearly different from that

of the AuGeNi contact. From the microstructural analysis, the carrier transport mechanism can be explained as follows.

Since the conduction band discontinuity was reported to be ~0.06 eV at the (100)GaAs/epitaxial-Ge interface,²³ the voltage drop at the GaAs/Ge interface is negligibly small. Therefore, there are two energy barriers to limit the electron transport through these interfaces; one is the energy barrier (ϕ_B) between the metal and the heavily doped n⁺⁺-GaAs or n⁺⁺-Ge layer, and the other is the energy barrier (ϕ_0) between the n⁺⁺-GaAs and n⁺-GaAs layers. If the R_c value is limited by the electron transport through the barrier at the metal/n⁺⁺-GaAs or metal/n⁺⁺-Ge interface, the R_c value is dominated by field emission mechanism²⁴ and is insensitive to the temperature. Therefore, the transport through the barrier at the n⁺-GaAs/n⁺⁺-GaAs interface would be dependent on temperatures. Based on the model proposed by Lønnum and Johannessen,²⁵ the barrier ϕ_0 appears from the nonuniform doping distribution in the GaAs substrate by ion implantation. Figure 13 shows the energy band diagrams at the (a) metal/GaAs and at the (b) metal/Ge/GaAs interface, together with the doping concentration profiles formed as a sum of the Si ion implantation and the heavily doped layer. They showed that assuming the Si doping profile of the LSS model,²⁶ the ϕ_0 value was minimized when the n⁺⁺-GaAs layer contact to the n⁺-GaAs at a depth of R_p (which corresponds to the depth of the maximum Si concentration and ~80 nm in the present condition). For the conventional AuGeNi contact, it was reported that large protrusions of the NiAs(Ge) phases with a depth of 100~200 nm were formed below the GaAs surface after contact formation,²⁻⁴ which indicates the formation of n⁺/n⁺⁺-GaAs junction at various depths. The junction depth (d) which controls the main current transport is believed to be nearly equal to the R_p value, which makes the ϕ_0 value negligibly small. For the present NiGe-based contact, the ϕ_0 value is expected to be larger due to the shallow junction depth (below 20 nm) less than the R_p value (seen in Fig. 13). Therefore, the R_c values of the

NiGe-based contacts are dominated by thermionic field emission mechanism²⁴ to transport through the barrier at the n^+/n^{++} homojunction interface and are sensitive to the temperatures because the tunneling probability is sensitive to the thermal energy of electrons.

COMPARISON AMONG NiGe-BASED OHMIC CONTACTS

The properties of the conventional AuGeNi contact¹⁻⁴ and NiGe contacts with or without third elements^{7,12-14} are summarized in Table I. Addition of the "direct" or "indirect" doping elements to the NiGe contacts succeeded in the reduction of the R_c values down to 0.3 Ω mm by forming the heavily doped layer at the metal/GaAs interface. These contacts provided the smooth surface and shallow reaction depth. Especially, the NiGe(Pd) contacts provided the lowest R_c values of 0.1 Ω mm and the reaction depth was by a factor of ~ 10 smaller than that of the conventional AuGeNi contacts. However, the NiGe(Pd) contacts were not thermally stable during annealing at 400°C. On the other hand, the NiGe(Te) contact with the R_c value of 0.2 Ω mm provided good thermal stability at 400°C which could be due to absence of low melting point compounds in the heavily doped layer at the metal/GaAs interface. In addition, the NiGe(In) contact¹⁴ with the R_c value of 0.3 Ω mm provided excellent thermal stability at 400°C. Further research is needed to prepare the ohmic contacts which have the R_c values less than 0.1 Ω mm and excellent thermal stability at 400°C.

CONCLUSION

In the present paper, NiGe-based ohmic contacts were studied systematically. Formation mechanism of NiGe ohmic contacts was investigated by correlating the electrical properties to the interfacial microstructure in order to obtain a guideline for reduction of the contact resistance. The NiGe contacts were found to have two different ohmic contact formation mechanisms. For the contacts with low Ge concentrations, n^{++} -regrown GaAs layers played a key role for the carrier transport through the interface between metal and n^+ -GaAs substrate. For the contacts with high Ge concentrations, thin n^+ -Ge layers grown epitaxially on the n^{++} -GaAs layers influenced significantly the current transport of the NiGe ohmic contacts. These results suggest that facilitating additional doping at the GaAs surface and/or in the epitaxially grown Ge layer is very effective for the R_c reduction. Based on this guideline, the effects of a small amount of third element addition to NiGe ohmic contacts were investigated. The third elements were direct doping elements (Sn, Sb, and Te), indirect doping elements (Pd, Pt, Au, Ag, and Cu), and low barrier forming element (In). The contact resistances (R_c) of the NiGe contacts were reduced to less than 0.3 Ω mm by adding a third element with ~ 6 nm thickness. These contacts had smooth surface and shallow reaction depth. The reduction of R_c values was found

to be due to heavy doping of Ge, Sn, or Te atoms at the GaAs surface, or due to formation of an epitaxial n^{++} -Ge or n^+ - $\text{In}_x\text{Ga}_{1-x}$ As layer between metal and the n^{++} -GaAs layers. These results indicate that addition of the direct doping element or the indirect doping element is very effective to reduce the R_c value of the NiGe contacts. The guideline for the R_c reduction presented in this paper would be applicable to other compound semiconductors such as GaN, ZnSe, and InP.

ACKNOWLEDGMENTS

The authors would like to acknowledge K. Yoshida, Department of Nuclear Engineering, Kyoto University for RBS measurement. This work was partly supported by an Aid for Scientific Research from the Ministry of Education, Science, and Culture, Japan.

REFERENCES

1. N. Braslau, J.B. Gunn and J.L. Staples, *Solid-State Electron.* 10, 381 (1967).
2. M. Murakami, K.D. Childs, J.M. Baker and A. Callegari, *J. Vac. Sci. Technol. B* 4, 903 (1986).
3. Y.C. Shih, M. Murakami, E.L. Wilkie and A. Callegari, *J. Appl. Phys.* 62, 582 (1987).
4. M. Murakami, *Mater. Sci. Rep.* 5, 273 (1990).
5. K. Ohta and M. Ogawa, *Ext. Abs., Jpn. Soc. Appl. Phys.* 35(2), 263 (1974).
6. W.T. Anderson, Jr, A. Christo and J.E. Davey, *IEEE J. Solid-St. Circuits* SC-13, 430 (1978).
7. K. Tanahashi, H.J. Takata, A. Otsuki and M. Murakami, *J. Appl. Phys.* 72, 4183 (1992).
8. E. Kolawa, W. Flick, C.W. Nieh, J.M. Molarius, M.A. Nicolet, J.L. Tandon, J.H. Madok and F.C.T. So, *IEEE Trans. Electron Dev.* 36, 1223 (1989).
9. A.K. Sinha, T.E. Smith and H.J. Levinstein, *IEEE Trans. Electron Dev.* 22, 218 (1975).
10. E.D. Marshall, B. Zhang, L.C. Wang, P.F. Jiao, W.X. Chen, T. Sawada and S.S. Lau, *J. Appl. Phys.* 62, 942 (1987).
11. M.O. Aboelfotoh, S. Oktyabrsky, J. Narayan and J.M. Woodall, *J. Appl. Phys.* 76, 5760 (1994).
12. H.R. Kawata, T. Oku, A. Otsuki and M. Murakami, *J. Appl. Phys.* 75, 2530 (1994).
13. H. Wakimoto, T. Oku, Y. Koide and M. Murakami, submitted to *J. Electrochem. Soc.*
14. T. Oku, H. Wakimoto, A. Otsuki and M. Murakami, *J. Appl. Phys.* 75, 2522 (1994).
15. S.M. Sze, *Physics of Semiconductor Devices* (New York: Wiley Inter. Science, 1981), p. 850.
16. A.K. Nissen, F.R. de Boer, R. Boom, P.F. de Chatel, W.C.M. Mattens and A.R. Miedema, *CALPAD.* 7, 51 (1983).
17. W. Hume-Rothery and G.V. Raynor, *J. Inst. Metals* 61, 205 (1937).
18. M. Ogawa, *Thin Solid Films* 70, 181 (1980).
19. A. Lahav, M. Eizenberg and Y. Komem, *J. Appl. Phys.* 60, 991 (1986).
20. T. Sands, V.G. Keramidas, A.J. Yu, K-M. Yu, R. Gronsky and J. Washburn, *J. Mater. Res.* 2, 262 (1987).
21. T. Sands, V.G. Keramidas, R. Gronsky and J. Washburn, *Thin Solid Films* 136, 105 (1986).
22. E.D. Marshall, B. Zhang, L.C. Wang, P.F. Jiao, W.X. Chen, T. Sawada and S.S. Lau, *J. Appl. Phys.* 62, 942 (1987).
23. T. Fukada, T. Asano, S. Frukawa, and H. Ishiwara, *J. Appl. Phys.* 26, 117 (1987).
24. A.C.Y. Yu, *Solid-State Electron.* 13, 239 (1970).
25. F. Lønnum and J.S. Johannessen, *Electron. Lett.* 22, 632 (1986).
26. J. Linhard, M. Scharff and Schiøtt, *Mat. Fys. Medd. Dan. Vidensk. Selsk.* 33, 1 (1963).